Polynomial Matrix SVD Algorithms for Broadband Optical MIMO Systems

Andreas Ahrens[1], André Sandmann[1], Zeliang Wang[2] and John G. McWhirter[2]
[1]*Hochschule Wismar, University of Technology, Business and Design, Philipp-Müller-Straße 14, 23966, Wismar, Germany*
[2]*School of Engineering, Cardiff University, Queen's Buildings, The Parade, Cardiff, CF24 3AA, Wales, U.K.*

Keywords: Polynomial Matrix SVD, Broadband MIMO, Optical MIMO, Bit Allocation, Power Allocation.

Abstract: Polynomial matrix singular value decomposition (PMSVD) plays a very important role in broadband multiple-input multiple-output (MIMO) systems. It can be used to decompose a broadband MIMO channel matrix in order to recover the transmitted signals corrupted by the channel interference (CI) at the receiver. In this contribution newly developed singular value decomposition (SVD) algorithm for polynomial matrices are analyzed and compared in the application of decomposing optical MIMO channels. The bit-error rate (BER) performance is evaluated and optimized by applying bit and power allocation schemes. For our simulations, the specific impulse responses of the (2×2) MIMO channel, including a 1.4 km multi-mode fiber and optical couplers at both ends, are measured for the operating wavelength of 1576 nm.

1 INTRODUCTION

An explosive development of MIMO technology has been witnessed in wireless communication systems over the last decade. Compared to single-input single-output (SISO) systems, MIMO systems are capable of achieving higher data rates and transmission reliabilities. Aiming to increase the fiber capacity, the concept of MIMO in optical transmission systems has also attracted intensive research interests (Singer et al., 2008; Winzer and Foschini, 2011; Sandmann et al., 2016).

Theoretical investigations have shown that similar capacity increases are possible compared to wireless MIMO systems (Kühn, 2006; Tse and Viswanath, 2005). The basis for this approach is the exploitation of the different optical mode groups. However, the practical implementation has to cope with many technological obstacles such as mode multiplexing and management. This includes mode combining, mode maintenance and mode splitting. In order to improve existing simulation tools practical measurements are needed. That is why in this contribution a whole optical transmission testbed is characterized by its respective impulse responses obtained by high-bandwidth measurements.

In broadband MIMO systems, the channel is characterized by frequency-selective fading. In order to recover the transmitted data sequence corrupted by channel interference (CI), a conventional method is to combine the spatio-temporal vector coding (STVC) (Raleigh and Cioffi, 1998; Raleigh and Jones, 1999) with the SVD based equalization technique (Haykin, 2002). However, there are some existing papers (Ta and Weiss, 2007; Sandmann et al., 2015c) which discussed an alternative signal pre- and post-processing method used in broadband MIMO systems. Basically this method consists of two steps. The first step is based on the PMSVD which is used to remove the CI by decomposing the frequency-selective MIMO channel into a number of independent frequency-selective SISO channels, and the second step involves removing the remaining inter-symbol interference (ISI), which can be implemented by further equalization techniques, such as zero-forcing (ZF) equalization or maximum likelihood sequence estimations (MLSE). Whereas STVC-based approaches require guard intervals between consecutive data blocks, they can be avoided when PMSVD-based approaches are applied (Raleigh and Cioffi, 1998; McWhirter and Baxter, 2004; Wang et al., 2016).

The PMSVD method in most of the existing literature is computed by an iterative polynomial matrix eigenvalue decomposition (PEVD) algorithm, called the second order sequential best rotation (SBR2) algorithm (McWhirter et al., 2007). However, there are some other PEVD algorithms which have been developed recently, including the sequential matrix diago-

Ahrens, A., Sandmann, A., Wang, Z. and McWhirter, J.
Polynomial Matrix SVD Algorithms for Broadband Optical MIMO Systems.
DOI: 10.5220/0005949400350042
In *Proceedings of the 13th International Joint Conference on e-Business and Telecommunications (ICETE 2016) - Volume 3: OPTICS*, pages 35-42
ISBN: 978-989-758-196-0

nalization (SMD) algorithm (Redif et al., 2015), multiple shift maximum element SMD (MSME-SMD) algorithm (Corr et al., 2014), and multiple shift SBR2 (MS-SBR2) algorithm (Wang et al., 2015) etc. All these PEVD algorithms can provide much faster convergence than the SBR2 algorithm.

The contribution of this paper is to investigate different PEVD algorithms in computing the PMSVD for broadband optical MIMO systems. The resulting CI after decomposition, which is indicated by the diagonalization level, is also examined among different PEVD algorithms. In particular, the possible errors caused by the proposed PMSVD method are also discussed. In addition, transmission and power allocation schemes are employed to bring further improvement in BER performance. Our simulations are implemented based on a measured (2×2) optical MIMO channel which comprises a 1.4 km multi-mode fiber and optical couplers at both ends, and the channel impulse responses are measured for the operating wavelength of 1576 nm (Sandmann et al., 2015a; Sandmann et al., 2015c).

The rest of the paper is structured as follows. The MIMO channel model with polynomial matrix representation is introduced in Sec. 2. In Sec. 3 we describe the concept of broadband MIMO channel decomposition, i. e. PMSVD. Sec. 4 presents some existing iterative PEVD algorithms for calculating the PMSVD. The underlying MIMO testbed is presented in Sec. 5. Simulation results and conclusions are shown in Sec. 6 and Sec. 7, respectively.

2 MIMO CHANNEL MODEL

Given a frequency selective optical MIMO link with n_{T} optical inputs and n_{R} optical outputs, the channel can be modelled as a polynomial matrix with an indeterminate variable z^{-1} given by

$$\underline{\mathbf{C}}(z)=\sum_{\tau=0}^{T}\mathbf{C}(\tau)z^{-\tau}=\begin{bmatrix}\underline{c}_{11}(z) & \cdots & \underline{c}_{1n_{\mathrm{T}}}(z)\\ \vdots & \ddots & \vdots\\ \underline{c}_{n_{\mathrm{R}}1}(z) & \cdots & \underline{c}_{n_{\mathrm{R}}n_{\mathrm{T}}}(z)\end{bmatrix}, \tag{1}$$

where $\mathbf{C}(\tau)\in\mathbb{C}^{n_{\mathrm{R}}\times n_{\mathrm{T}}}$ denotes the polynomial coefficient matrix at time lag τ and $\underline{c}_{\nu\mu}(z)$ is the polynomial matrix entity which represents the channel impulse response between the μ-th optical input and the ν-th optical output. It takes the form of

$$\underline{c}_{\nu\mu}(z)=\sum_{\tau=0}^{T}c_{\nu\mu}(\tau)z^{-\tau}, \tag{2}$$

where $c_{\nu\mu}(\tau)$ denotes a non-zero element of the symbol rate sampled overall channel impulse response at the τ-th lag. In this case there are $T+1$ lags in total for each SISO channel.

Throughout this paper, polynomial matrices and vectors are denoted as underscored boldface letters. Finally, the resulting MIMO system model can be described in polynomial matrix notation as follows

$$\underline{\mathbf{x}}(z)=\underline{\mathbf{C}}(z)\underline{\mathbf{s}}(z)+\underline{\mathbf{n}}(z), \tag{3}$$

where $\underline{\mathbf{x}}(z)$, $\underline{\mathbf{s}}(z)$ and $\underline{\mathbf{n}}(z)$ represent the received signal, the source signal and the noise signal in z-domain respectively (Sandmann et al., 2015c).

3 BROADBAND MIMO CHANNEL DECOMPOSITION VIA PMSVD

Given the MIMO channel matrix $\underline{\mathbf{C}}(z)$ as shown in (1), the CI can be removed by performing the PMSVD, which can be expressed as (McWhirter and Baxter, 2004)

$$\underline{\mathbf{C}}(z)=\widetilde{\underline{\mathbf{U}}}(z)\underline{\mathbf{\Sigma}}(z)\underline{\mathbf{V}}(z)=\widetilde{\underline{\mathbf{U}}}(z)\begin{bmatrix}\underline{\mathbf{\Gamma}}(z)\\ 0\end{bmatrix}\underline{\mathbf{V}}(z), \tag{4}$$

where we assume $n_{\mathrm{R}}\geq n_{\mathrm{T}}$, and $\underline{\mathbf{\Gamma}}(z)$ is a diagonal polynomial matrix with $n=n_{\mathrm{T}}$ diagonal elements, s.t. $\underline{\mathbf{\Gamma}}(z)=\mathrm{diag}\{\underline{\gamma}_1(z),\underline{\gamma}_2(z),\cdots,\underline{\gamma}_n(z)\}$. $\widetilde{\underline{\mathbf{U}}}(z)$ and $\underline{\mathbf{V}}(z)$ are paraunitary polynomial matrices with dimension $n_{\mathrm{R}}\times n_{\mathrm{R}}$ and $n_{\mathrm{T}}\times n_{\mathrm{T}}$ respectively, s.t. $\widetilde{\underline{\mathbf{U}}}(z)\underline{\mathbf{U}}(z)=\underline{\mathbf{U}}(z)\widetilde{\underline{\mathbf{U}}}(z)=\mathbf{I}_{n_{\mathrm{R}}}$ and $\widetilde{\underline{\mathbf{V}}}(z)\underline{\mathbf{V}}(z)=\underline{\mathbf{V}}(z)\widetilde{\underline{\mathbf{V}}}(z)=\mathbf{I}_{n_{\mathrm{T}}}$. Here the notation $\widetilde{\ }$ over the polynomial matrix $\underline{\mathbf{U}}(z)$ denotes the paraconjugate operation which is computed by performing Hermitian transpose $\{\cdot\}^{\mathrm{H}}$ of all the polynomial coefficient matrices $\mathbf{U}(\tau)$ and time-reversing all entries inside, i.e. $\widetilde{\underline{\mathbf{U}}}(z)=\underline{\mathbf{U}}^{\mathrm{H}}(1/z)$.

Note that $\widetilde{\underline{\mathbf{U}}}(z)$ and $\underline{\mathbf{V}}(z)$ are acting as the multichannel all-pass filters which can transform the frequency-selective MIMO channel into a number of independent frequency selective SISO channels while still preserving the total signal energy (Vaidyanathan, 1993).

In this paper, the PMSVD in (4) is implemented by calculating the PEVD of two polynomial matrices $\underline{\mathbf{C}}(z)\widetilde{\underline{\mathbf{C}}}(z)$ and $\widetilde{\underline{\mathbf{C}}}(z)\underline{\mathbf{C}}(z)$, which take the form as

$$[\underline{\mathbf{C}}(z)\widetilde{\underline{\mathbf{C}}}(z)]_{n_{\mathrm{R}}\times n_{\mathrm{R}}}=\widetilde{\underline{\mathbf{U}}}(z)\underline{\mathbf{\Sigma}}(z)\widetilde{\underline{\mathbf{\Sigma}}}(z)\underline{\mathbf{U}}(z), \tag{5}$$

and

$$[\widetilde{\underline{\mathbf{C}}}(z)\underline{\mathbf{C}}(z)]_{n_{\mathrm{T}}\times n_{\mathrm{T}}}=\widetilde{\underline{\mathbf{V}}}(z)\widetilde{\underline{\mathbf{\Sigma}}}(z)\underline{\mathbf{\Sigma}}(z)\underline{\mathbf{V}}(z). \tag{6}$$

Further details about PEVD algorithms will be discussed in the following section. To eliminate the CI, the transmit data vector $\underline{\mathbf{s}}(z)$ is pre-multiplied by $\widetilde{\underline{\mathbf{V}}}(z)$

at the transmitter, and pre-multiplied by $\underline{\mathbf{U}}(z)$ at the receiver, which results in

$$\underline{\mathbf{x}}(z) = \underline{\mathbf{\Sigma}}(z)\underline{\mathbf{s}}(z) + \underline{\mathbf{w}}(z), \tag{7}$$

where $\underline{\mathbf{w}}(z) = \underline{\mathbf{U}}(z)\underline{\mathbf{n}}(z)$. Note that neither the transmit power is increased, nor the channel noise is enhanced here.

Unlike the conventional SVD-based method, each diagonal element (also called layer) in $\underline{\mathbf{\Sigma}}(z)$ is frequency-selective and hence ISI occurs. In order to remove the ISI, layer-specific T-spaced zero forcing equalizers (Sandmann et al., 2015c) are adopted in this paper.

4 ITERATIVE PEVD ALGORITHMS

As mentioned above, the PEVD method can be used to formulate the PMSVD problem in equation (4), and the idea of PEVD has been generalized as (McWhirter et al., 2007)

$$\underline{\mathbf{H}}(z)\underline{\mathbf{R}}(z)\widetilde{\underline{\mathbf{H}}}(z) \approx \underline{\mathbf{D}}(z), \tag{8}$$

where $\underline{\mathbf{R}}(z)$ is assumed to be a $M \times M$ input para-Hermitian matrix, such that $\widetilde{\underline{\mathbf{R}}}(z) = \underline{\mathbf{R}}(z)$, $\underline{\mathbf{H}}(z)$ is a paraunitary matrix which aims to diagonalize $\underline{\mathbf{R}}(z)$ by means of paraunitary similarity transformation, and $\underline{\mathbf{D}}(z)$ is (ideally) a diagonal matrix.

This is an iterative process which transforms all the off-diagonal elements in $\underline{\mathbf{R}}(z)$ onto the diagonal subject to the pre-specified stop condition. For the remaining part of this section, different PEVD algorithms are briefly reviewed.

4.1 The SBR2 Algorithm

At the i-th iteration, the SBR2 algorithm (McWhirter et al., 2007) starts by locating the maximum off-diagonal element $r_{jk}^{(i)}(\tau)$. To find the maximum off-diagonal element, we define a matrix $\mathbf{S}^{(i)}(\tau)$, which contains only the upper triangular elements in $\mathbf{R}^{(i-1)}(\tau)$ with the remaining elements set to zero. Thus the location of $r_{jk}^{(i)}(\tau)$, $(j < k)$ found at i-th iteration satisfies

$$\{j^{(i)}, k^{(i)}, \tau^{(i)}\} = \arg\max_{j,k,\tau} \|\mathbf{S}^{(i)}(\tau)\|_{\infty}, \tag{9}$$

where $j^{(i)}$, $k^{(i)}$ and $\tau^{(i)}$ are the corresponding row, column and time lag index. An elementary delay matrix $\underline{\mathbf{P}}^{(i)}(z)$ and Jacobi rotation $\mathbf{Q}^{(i)}$ are applied to bring $r_{jk}^{(i)}(\tau)$ and its complex conjugate $r_{kj}^{(i)}(-\tau)$ onto the zero-lag ($\tau = 0$) coefficient matrix $\mathbf{R}^{(i-1)}(0)$, and then rotate its energy onto the diagonal. This results in $\underline{\mathbf{R}}^{(i)}(z)$ given by

$$\underline{\mathbf{R}}^{(i)}(z) = \mathbf{Q}^{(i)}\underline{\mathbf{P}}^{(i)}(z)\underline{\mathbf{R}}^{(i-1)}(z)\widetilde{\underline{\mathbf{P}}}^{(i)}(z)\mathbf{Q}^{\mathrm{H}(i)}. \tag{10}$$

Then the elementary paraunitary matrix $\underline{\mathbf{E}}^{(i)}(z)$ can be expressed as

$$\underline{\mathbf{E}}^{(i)}(z) = \mathbf{Q}^{(i)}\underline{\mathbf{P}}^{(i)}(z). \tag{11}$$

The algorithm continues its iterative process until all the off-diagonal elements are smaller than a given threshold ε which can be set to a very small value to achieve sufficient accuracy. Assuming that the algorithm has converged at the N-th iteration, the diagonalized para-Hermitian matrix in (8) takes the form of

$$\underline{\mathbf{D}}(z) = \mathrm{diag}\{\underline{d}_1(z), \underline{d}_2(z), \cdots, \underline{d}_M(z)\}, \tag{12}$$

and the generated paraunitary polynomial matrix is given by

$$\underline{\mathbf{H}}(z) = \prod_{i=1}^{N} \underline{\mathbf{E}}^{(i)}(z) = \underline{\mathbf{E}}^{(N)}(z) \cdots \underline{\mathbf{E}}^{(2)}(z)\underline{\mathbf{E}}^{(1)}(z). \tag{13}$$

4.2 The SMD Algorithm

Unlike the SBR2 algorithm, the sequential matrix diagonalization (SMD) algorithm (Redif et al., 2015) requires a initialization step to diagonalize the zero-lag coefficient matrix $\mathbf{R}^{(0)}(0)$ before all iterations. This is implemented by computing a full EVD to $\mathbf{R}^{(0)}(0)$ and then applying the corresponding modal matrix to the rest of coefficient matrices $\mathbf{R}^{(0)}(\tau), \tau \neq 0$. For the i-th iteration, it starts by locating the column that contains the maximum off-diagonal energy, and then according to the location information $k^{(i)}$ and $\tau^{(i)}$, it shifts the corresponding row and column pair onto the zero-lag coefficient matrix. As to the rotation step, rather than just using a single Jacobi rotation as with SBR2, the SMD algorithm computes a full EVD for the shifted zero-lag coefficient matrix $\mathbf{R}'^{(i)}(0)$.

4.3 The MSME-SMD Algorithm

The MSME-SMD algorithm (Corr et al., 2014) introduced a distinguishing search and shift strategy, which can transfer more off-diagonal elements than both SBR2 and SMD onto the diagonal at each iteration. For each iteration, more than one maximum off-diagonal element is found by using a reduced search space strategy. Every row and column pair containing a maximum off-diagonal element will then be shifted to the zero-lag coefficient matrix. This is different to

the way the SMD algorithm operates. The SMD algorithm always shifts the row and column pair containing the maximum off-diagonal energy rather than the maximum off-diagonal element as in MSME-SMD. At the rotation step, the MSME-SMD algorithm follows the same procedure as the SMD algorithm transferring all the off-diagonal elements in $\mathbf{R}'^{(i)}(0)$ onto the diagonal.

4.4 The MS-SBR2 Algorithm

The MS-SBR2 algorithm (Wang et al., 2015) is an improved version of the SBR2 algorithm in terms of the algorithm convergence speed. Basically it adopts the advantages of less computational cost from SBR2 and the faster convergence from MSME-SMD, which seems to provide a compromise between the SBR2 and the SMD algorithm family. The MS-SBR2 algorithm uses a distinguishing search strategy of the off-diagonal elements which is akin to that of the MSME-SMD algorithm, so that it can achieve the diagonalization with less iterations than the SBR2 algorithm. For the i-th iteration, the MS-SBR2 algorithm involves multiple shifts operations $\widehat{\underline{\mathbf{P}}}^{(i)}(z)$, followed by a sequence of Jacobi rotations $\widehat{\mathbf{Q}}^{(i)}$. Therefore, the resulting para-Hermitian matrix is computed by

$$\underline{\mathbf{R}}^{(i)}(z) = \widehat{\mathbf{Q}}^{(i)}\widehat{\underline{\mathbf{P}}}^{(i)}(z)\underline{\mathbf{R}}^{(i-1)}(z)\widetilde{\widehat{\underline{\mathbf{P}}}}^{(i)}(z)\widehat{\mathbf{Q}}^{\mathrm{H}(i)}, \quad (14)$$

where $\widehat{\underline{\mathbf{P}}}^{(i)}(z) = \prod_{l=1}^{L^{(i)}}\underline{\mathbf{P}}^{(l,i)}(z)$, $\widehat{\mathbf{Q}}^{(i)} = \prod_{l=1}^{L^{(i)}}\mathbf{Q}^{(l,i)}$ and $L^{(i)}$ denotes the total number of off-diagonal elements shifted to the zero-lag coefficient matrix at the i-th iteration. Accordingly the elementary paraunitary matrix can be expressed as $\widehat{\underline{\mathbf{E}}}^{(i)}(z) = \widehat{\mathbf{Q}}^{(i)}\widehat{\underline{\mathbf{P}}}^{(i)}(z)$. Note that when $L^{(i)} = 1$, the MS-SBR2 algorithm is identical to the SBR2 algorithm.

Different PEVD algorithms are assessed in terms of the normalized remaining off-diagonal energy at the i-th iteration. This is defined as

$$\eta^{(i)} = \frac{\sum_\tau \sum_{m,n=1,m\neq n}^{M} |r_{mn}^{(i)}(\tau)|^2}{\sum_\tau \|\mathbf{R}(\tau)\|_{\mathrm{F}}^2}, \quad (15)$$

where the notation $\|\cdot\|_{\mathrm{F}}$ denotes the Frobenius norm.

The comparison among different PEVD algorithms is calculated via Monte Carlo simulations over an ensemble of 100 different (6×6) para-Hermitian matrices $\underline{\mathbf{R}}(z)$ of order 13, which is generated from matrices $\underline{\mathbf{A}}(z) \in \underline{\mathbb{C}}^{6\times 6}$ of order 7 with i.i.d. zero mean unit variance complex Gaussian entries, s.t. $\underline{\mathbf{R}}(z) = \underline{\mathbf{A}}(z)\widetilde{\underline{\mathbf{A}}}(z)$. Fig. 1 shows the normalized remaining off-diagonal energy $\eta^{(i)}$ versus iteration index i for each PEVD algorithm. Obviously, both the SMD and MSME-SMD algorithms outperform SBR2 and MS-SBR2 in terms of eliminating the off-diagonal energy. This is due to the fact that a full EVD operation is applied in SMD algorithm family at each iteration, which can transform more off-diagonal elements onto diagonal. However, this is also one of the factors which causes the SMD algorithm family much higher computational cost than the SBR2 algorithm. Obviously the MS-SBR2 algorithm requires much fewer iterations than the conventional SBR2 algorithm to achieve the same level of diagonalization. However, it should also be noticed that each iteration within MS-SBR2 involves more rotation steps, which means the computational costs between them are comparable. Nonetheless, the MS-SBR2 algorithm has been found to converge faster than SBR2 especially when decomposing high dimension para-Hermitian polynomial matrices. For further details of the algorithm, including numerical examples and proof of convergence, see (Wang et al., 2015).

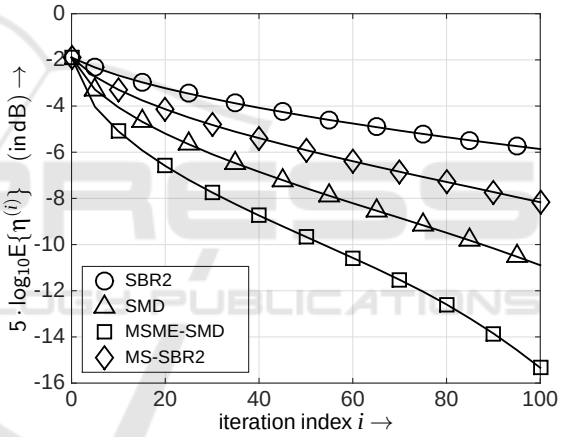

Figure 1: Comparisons of normalized off-diagonal energy among different PEVD algorithms, showing ensemble averages versus iterations.

As shown by the simulation results, the off-diagonal energy with the use of the investigated PEVD algorithms becomes neglectable small at a sufficiently high number of iterations.

4.5 Accuracy of the Decomposition

There are two main factors which can affect the accuracy of the decomposition. Firstly, since the decomposition is performed upon the two para-Hermitian matrices $\underline{\mathbf{C}}(z)\widetilde{\underline{\mathbf{C}}}(z)$ and $\widetilde{\underline{\mathbf{C}}}(z)\underline{\mathbf{C}}(z)$ as shown in equations (5) and (6), the resulting diagonal matrix $\underline{\mathbf{\Sigma}}(z)$ might be less accurate than that found by the way of operating the decomposition directly upon the channel matrix $\underline{\mathbf{C}}(z)$.

Secondly, for the broadband MIMO application,

a strictly diagonalized channel matrix is required. However, the proposed PMSVD method can only generate an approximately diagonal matrix subject to the pre-specified stop condition of the algorithm, so there will be errors when assuming all off-diagonal elements of the matrix $\underline{\mathbf{\Sigma}}(z)$ are equal to zero. In addition, due to the fact that the orders of the polynomial matrices increase as the iteration goes throughout the PEVD process, proper truncations are usually required for the matrices $\underline{\mathbf{U}}(z)$, $\underline{\mathbf{\Sigma}}(z)$, and $\underline{\mathbf{V}}(z)$ in order to keep orders as small as possible and reduce the computational cost of the algorithm. This can cause a very small proportion of the total Frobenius norm of the matrix being eliminated, which also can bring errors.

5 OPTICAL MIMO TESTBED

An optical MIMO system can be formed by feeding different sources of light into the fibre, which can activate different optical mode groups. This can be carried out by using centric and eccentric light launching conditions and subsequent combining of the activated different mode groups with a fusion coupler as shown in Fig. 2 (Sandmann et al., 2014).

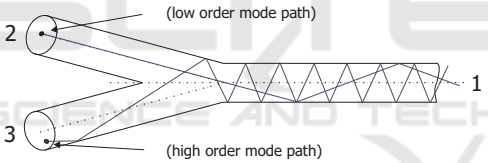

Figure 2: Transmitter side fusion coupler for launching different sources of light into the MMF.

Different sources of light lead to different power distribution patterns at the fibre end depending on the transmitter side light launch conditions. Fig. 3 highlights the measured mean power distribution pattern at the end of a 1.4 km multi-mode fibre (MMF). Here, for splitting the different mode groups a similar fusion coupler is used.

The measurement setup depicted in Fig. 4 shows the testbed with the utilized devices for measuring the system properties of the optical MIMO channel in form of its specific impulse responses needed for modelling the MIMO data transmission.

A picosecond laser unit is chosen for generating the 25 ps input pulse. This input pulse is used to measure separately the different SISO channels within the MIMO system. Since the used picosecond laser unit doesn't guarantee a fully flat frequency spectrum in the region of interest, the captured signals have to be deconvolved (Sandmann et al., 2013). The obtained impulse responses are forming the base for modelling the MIMO transmission system. Fig. 5 highlights the resulting electrical MIMO system model.

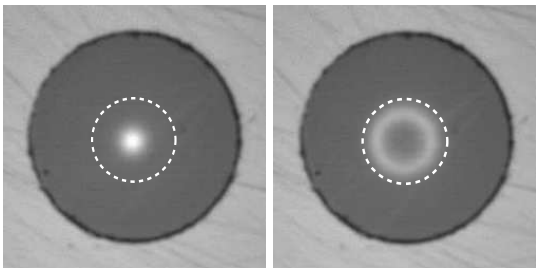

Figure 3: Measured mean power distribution pattern when using the fusion coupler at the transmitter side (left: centric mode excitation; right: eccentric mode excitation); the dotted line represents the 50 µm core size.

6 SIMULATION RESULTS

In this work, the BER quality is studied by using fixed transmission modes with a spectral efficiency of 8 bit/s/Hz. The analyzed quadrature amplitude modulation (QAM) constellations, equivalent to how many bits are allocated to each layer, are shown in Tab. 1.

Table 1: Transmission Modes.

throughput	layer 1	layer 2
8 bit/s/Hz	256	0
8 bit/s/Hz	64	4
8 bit/s/Hz	16	16

The channel, studied in this contribution, is a measured (2×2) optical MIMO channel.

Here, the measurement results within a 1.4 km (2×2) optical MIMO channel at an operating wavelength of 1576 nm, depicted in Fig. 6, have been used (Sandmann et al., 2015b). The graphs clearly show the effect of chromatic dispersion being characteristic at this operating wavelength in a standard fiber.

Applying PMSVD to this frequency-selective MIMO channel results in layers having a time-dispersive characteristic and hence ISI occurs on each layer. The ISI is removed by applying a T-spaced zero forcing (ZF) equalizer and therefore this equalization scheme is entitled T-PMSVD. The equalizers modify the noise power on each layer differently, which is expressed by the weighting factors θ_ℓ, with ℓ denoting the layer index. These factors determine the layer specific SNRs and hence also the total BER performance (Sandmann et al., 2015c). Calculating the PMSVD of the optical MIMO channel using different PEVD algorithms shows that the weighting factors θ_ℓ listed in Tab. 2 are identical. This implies

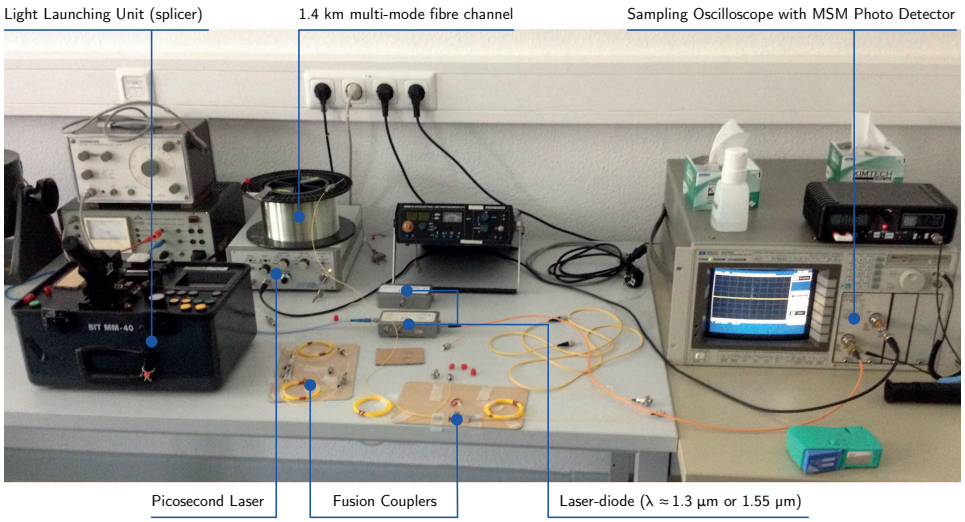

Figure 4: Measurement setup for determining the MIMO specific impulse responses.

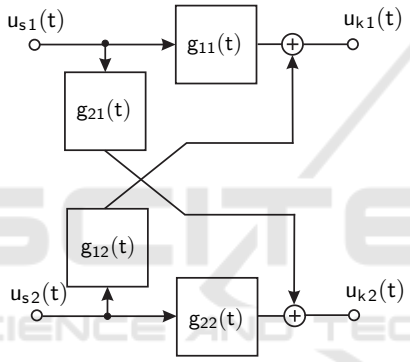

Figure 5: Electrical (2×2) MIMO system model (example: $n_R = n_T = 2$).

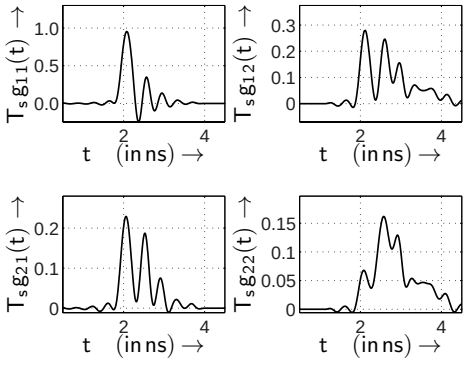

Figure 6: Measured electrical MIMO impulse responses with respect to the pulse frequency $f_T = 1/T_s = 620$ MHz at 1576 nm operating wavelength.

that the achievable BER is independent of the applied PEVD algorithms for the studied (2×2) MIMO channel. In addition, the remaining off-diagonal energy $\varepsilon = \sum_\tau \|\mathbf{C}(\tau)\|_F^2 - \sum_\tau \|\mathbf{\Sigma}(\tau)\|_F^2$ is negligibly small,

Table 2: Comparisons of remaining off-diagonal energy ε and noise amplification factor θ_ℓ among different PEVD algorithms, showing that different PEVD algorithms can achieve exactly the same BER performance subject to the same stop criterion of the PEVD algorithms, i. e. the threshold of the off-diagonal element $\varepsilon = 10^{-4}$.

algorithms	ε	θ_1	θ_2
SBR2	1.26×10^{-6}	37.22	4243.46
SMD	1.26×10^{-6}	37.22	4243.46
MSME-SMD	1.26×10^{-6}	37.22	4243.46
MS-SBR2	1.26×10^{-6}	37.22	4243.46

which means that the CI has been significantly eliminated.

The BER performance results, obtained by applying the SBR2 algorithm for calculating the PMSVD, are depicted in Fig. 8 for the different QAM constellation sizes. The $(256,0)$ transmission scheme shows the best performance results suggesting that not all layers should be activated when optimizing the BER performance.

Based on the unequal weighting of the layers, PA can be used to balance the bit-error probabilities in the different numbers of activated MIMO layers. Regarding the channel quality, the BER performance is affected by the layer-specific weighting factors, the chosen QAM-constellation size as well as the layer-specific noise power. Since optimal PA solutions are notably computationally complex to implement, a suboptimal solution which concentrates on the argument of the complementary error function is investigated in this work (Ahrens et al., 2015).

By applying T-PMSVD the ISI is fully removed by the equalizer and thus for each layer the half vertical eye opening of the receive signal equals the

half-level amplitude of the transmitted symbols. The drawback of the T-PMSVD is that the noise and hence the noise power is weighted differently on each layer by the equalizer coefficients expressed by the factors θ_1 and θ_2 as shown in Tab. 2. The proposed PA algorithm distributes the available transmit power such that the layer specific SNRs are equal (Sandmann et al., 2015c; Ahrens et al., 2015). The resulting SNRs for the proposed PA scheme in T-PMSVD systems are visualized in Fig. 7.

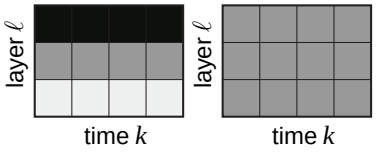

Figure 7: Illustration of the remaining SNRs in T-PMSVD systems without applying PA (left) and with layer-based PA (right). The color black refers to high and white to low SNR values.

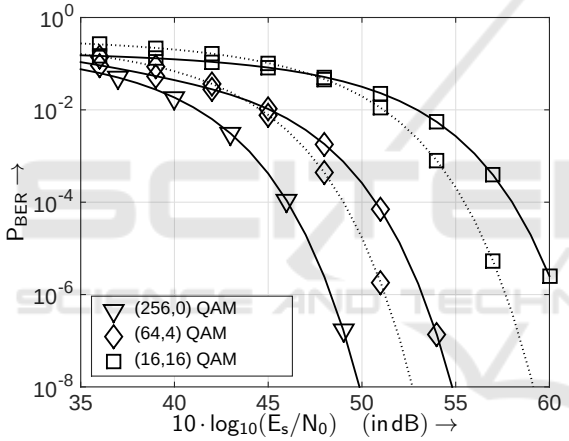

Figure 8: BER with PA (dotted line) and without PA (solid line) by applying the T-PMSVD equalization scheme, showing the comparisons among different transmission modes when transmitting over the optical (2×2) MIMO channel.

7 CONCLUSION

We have investigated the PMSVD technique in the application of decomposing the channel matrix of a measured (2×2) optical MIMO system, and different iterative PEVD algorithms have been utilized for the calculation of PMSVD. Despite the different number of iterations needed to minimize the off-diagonal element below a given threshold, all investigated PEVD algorithms show the same BER performance.

ACKNOWLEDGEMENTS

This work has been funded by the German Ministry of Education and Research (No. 03FH016PX3).

REFERENCES

Ahrens, A., Sandmann, A., Lochmann, S., and Wang, Z. (2015). Decomposition of Optical MIMO Systems using Polynomial Matrix Factorization. In *2nd IET International Conference on Intelligent Signal Processing (ISP)*, London (United Kingdom).

Corr, J., Thompson, K., Weiss, S., McWhirter, J. G., Redif, S., and Proudler, I. K. (2014). Multiple Shift Maximum Element Sequential Matrix Diagonalisation for Parahermitian Matrices. In *IEEE SSP Workshop*, pages 312–315, Gold Coast (Australia).

Haykin, S. S. (2002). *Adaptive Filter Theory.* Prentice Hall, New Jersey.

Kühn, V. (2006). *Wireless Communications over MIMO Channels – Applications to CDMA and Multiple Antenna Systems.* Wiley, Chichester.

McWhirter, J. G. and Baxter, P. D. (2004). A Novel Technique for Broadband Singular Value Decomposition. In *12th Annual ASAP Workshop*, MA (USA).

McWhirter, J. G., Baxter, P. D., Cooper, T., Redif, S., and Foster, J. (2007). An EVD Algorithm for Para-Hermitian Polynomial Matrices. *IEEE Trans. SP*, 55(5):2158–2169.

Raleigh, G. G. and Cioffi, J. M. (1998). Spatio-Temporal Coding for Wireless Communication. *IEEE Transactions on Communications*, 46(3):357–366.

Raleigh, G. G. and Jones, V. K. (1999). Multivariate Modulation and Coding for Wireless Communication. *IEEE Journal on Selected Areas in Communications*, 17(5):851–866.

Redif, S., Weiss, S., and McWhirter, J. G. (2015). Sequential Matrix Diagonalization Algorithms for Polynomial EVD of Parahermitian Matrices. *IEEE Trans. SP*, 61(1):81–89.

Sandmann, A., Ahrens, A., and Lochmann, S. (2013). Signal Deconvolution of Measured Optical MIMO-Channels. In *XV International PhD Workshop OWD*, pages 278–283, Wisla, Poland.

Sandmann, A., Ahrens, A., and Lochmann, S. (2014). Experimental Description of Multimode MIMO Channels utilizing Optical Couplers. In *ITG-Fachbericht 248: Photonische Netze*, pages 125–130, Leipzig (Germany). VDE VERLAG GmbH.

Sandmann, A., Ahrens, A., and Lochmann, S. (2015a). Modulation-Mode and Power Assignment in SVD-Assisted Broadband MIMO Systems using Polynomial Matrix Factorization. *Przeglad Elektrotechniczny*, 04/2015:10–13.

Sandmann, A., Ahrens, A., and Lochmann, S. (2015b). Performance Analysis of Polynomial Matrix SVD-based

Broadband MIMO Systems. In *Sensor Signal Processing for Defence Conference (SSPD)*, Edinburgh (United Kingdom).

Sandmann, A., Ahrens, A., and Lochmann, S. (2015c). Resource Allocation in SVD-Assisted Optical MIMO Systems using Polynomial Matrix Factorization. In *ITG-Fachbericht 257: Photonische Netze*, pages 128–134, Leipzig (Germany). VDE VERLAG GmbH.

Sandmann, A., Ahrens, A., and Lochmann, S. (2016). Experimental Evaluation of a (4x4) Multi-Mode MIMO System Utilizing Customized Optical Fusion Couplers. In *ITG-Fachbericht 249: Photonische Netze*, pages 101–105, Leipzig (Germany). VDE VERLAG GmbH.

Singer, A. C., Shanbhag, N. R., and Bae, H.-M. (2008). Electronic Dispersion Compensation– An Overwiew of Optical Communications Systems. *IEEE Signal Processing Magazine*, 25(6):110–130.

Ta, C. and Weiss, S. (2007). A Design of Precoding and Equalisation for Broadband MIMO Systems. In *Asilomar Conf. Signals, Systems & Computers*, pages 1616–1620, Pacific Grove, (CA).

Tse, D. and Viswanath, P. (2005). *Fundamentals of Wireless Communication*. Cambridge, New York.

Vaidyanathan, P. P. (1993). *Multirate Systems and Filter Banks*. Prentice Hall, New Jersey.

Wang, Z., McWhirter, J. G., Corr, J., and Weiss, S. (2015). Multiple Shift Second Order Sequential Best Rotation Algorithm for Polynomial Matrix EVD. In *23rd EUSIPCO*, pages 849–853, Nice (France).

Wang, Z., Sandmann, A., McWhirter, J., and Ahrens, A. (2016). Multiple Shift SBR2 Algorithm for Calculating the SVD of Broadband Optical MIMO Systems. In *39th International Conference on Telecommunications and Signal Processing (TSP)*, Vienna (Austria).

Winzer, P. J. and Foschini, G. J. (2011). MIMO Capacities and Outage Probabilities in Spatially Multiplexed Optical Transport Systems. *Optics Express*, 17(19):16680–16696.